RESEARCH ARTICLE | MAY 04 2022

Limited information of impedance spectroscopy about electronic diffusion transport: The case of perovskite solar cells

Agustín Bou ✉; Adam Pockett; Héctor Cruanyes; ... et. al

APL Mater 10, 051104 (2022)
https://doi.org/10.1063/5.0087705

Limited information of impedance spectroscopy about electronic diffusion transport: The case of perovskite solar cells

Cite as: APL Mater. 10, 051104 (2022); doi: 10.1063/5.0087705
Submitted: 8 February 2022 • Accepted: 14 April 2022 •
Published Online: 4 May 2022

Agustín Bou,[1,a)] Adam Pockett,[2] Héctor Cruanyes,[1] Dimitrios Raptis,[2] Trystan Watson,[2] Matthew J. Carnie,[2] and Juan Bisquert[1,a)]

AFFILIATIONS

[1] Institute of Advanced Materials (INAM), Universitat Jaume I, 12006 Castelló, Spain
[2] SPECIFIC, Materials Research Center, College of Engineering, Swansea University, Swansea SA1 8EN, United Kingdom

[a)] **Authors to whom correspondence should be addressed:** acatala@uji.es and bisquert@uji.es

ABSTRACT

Impedance Spectroscopy (IS) has proven to be a powerful tool for the extraction of significant electronic parameters in a wide variety of electrochemical systems, such as solar cells or electrochemical cells. However, this has not been the case with perovskite solar cells, which have the particular ionic-electronic combined transport that complicates the interpretation of experimental results due to an overlapping of different phenomena with similar characteristic frequencies. Therefore, the diffusion of electrons is indistinguishable on IS, and there appears the need to use other small perturbation experimental techniques. Here, we show that voltage-modulated measurements do not provide the same information as light-modulated techniques. We investigate the responses of perovskite solar cells to IS, Intensity-Modulated Photocurrent Spectroscopy (IMPS) and Intensity-Modulated Photovoltage Spectroscopy (IMVS). We find that the perturbations by light instead of voltage can uncover the electronic transport from other phenomena, resulting in a loop in the high-frequency region of the complex planes of the IMPS and IMVS spectra. The calculated responses are endorsed by the experimental data that reproduce the expected high frequency loops. Finally, we discuss the requirement to use a combination of small perturbation techniques for successful estimation of diffusion parameters of perovskite solar cells.

Impedance Spectroscopy (IS) has been a valuable technique for the analysis of the electrical response of a wide variety of semiconductor devices,[1–5] and specifically solar cells.[6,7] In fact, IS has led to the determination of carrier diffusion and recombination, charge transfer coefficient, and carrier lifetimes in silicon solar cells,[8] dye-sensitized solar cells,[9,10] and organic solar cells.[6,11] This important technique has also been widely used for the characterization of Perovskite Solar Cells (PSCs).[12–14] Although the IS characteristics of PSC display a rich diversity of features,[15] the interpretation of such spectra is not straightforward and the extraction of important parameters, such as the electronic carrier diffusion, has not been achieved.

One of the reasons for the complex interpretation of IS data on PSC is the influence of ionic motion inside the perovskite layer. The mobile ions can cause interface polarization,[16] affecting the charge transfer rates or inducing capacitive accumulation of electronic carriers. These phenomena affect the IS spectra, hindering the electronic information that is coupled with ionic phenomena and preventing the extraction of electronic information. However, the combination of IS and other small perturbation techniques has been demonstrated to be effective in the understanding of PSCs.[17–19] Recently, it was shown that electron diffusion parameters can be extracted from Intensity-Modulated Photocurrent Spectroscopy (IMPS).[20] However, this is not possible with voltage-modulated techniques such as IS.

Here, we aim to explain why voltage-modulated measurements do not have the same information as light-modulated techniques. For that purpose, we calculate the response of charge carrier diffusion for one voltage-modulated technique, the IS, and two light-modulated techniques, the IMPS and the Intensity-Modulated

Photovoltage Spectroscopy (IMVS). From these results, we conclude that while in IS, both the perturbation and the response take place at the same contact, in IMPS and IMVS, it is possible to apply the perturbation far from the collecting contact of one of the charge carriers, disclosing the diffusion of these particles along the film.

Following the methods that have been used for the calculation of the transfer functions of IS, IMPS, and IMVS,[20–23] we solve the conservation equation in the frequency domain. The equation for carrier density $n(x,t)$ including recombination and Beer–Lambert generation is as follows:

$$\frac{\partial n}{\partial t} = D_n \frac{\partial^2 n}{\partial x^2} - \frac{n - n_0}{\tau_n} + \alpha \Phi(t) e^{\alpha(x-d)}, \tag{1}$$

where D_n is the diffusion coefficient, n_0 is the equilibrium density under dark conditions, τ_n is the recombination lifetime, d is the active layer thickness, and α is the light absorption coefficient.

Since the solution has been already derived in the above-mentioned references, we skip the calculation details and directly show the solutions for the three techniques, in order to focus on the relationship between the solutions that provides new physical insight. We follow the notation used in Ref. 22, where the transfer functions have been expressed in terms of three characteristic frequency parameters that determine all possible spectral shapes. The solution of Eq. (1) in the frequency domain for the IS is

$$Z(\omega) = R_d \left(\frac{\omega_d}{p}\right)^{1/2} \coth\left(\left(\frac{p}{\omega_d}\right)^{1/2}\right), \tag{2}$$

where R_d is the diffusion resistance, p is defined as

$$p = i\omega + \omega_{rec}, \tag{3}$$

and the two characteristics frequencies are defined as

$$\omega_d = \frac{D_n}{d^2}, \tag{4}$$

$$\omega_{rec} = \tau_n^{-1}. \tag{5}$$

The solution of Eq. (1) in the frequency domain for the IMPS is

$$Q(\omega) = \frac{F(\omega)}{\cosh\left[\left(\frac{p}{\omega_d}\right)^{1/2}\right]}, \tag{6}$$

and for IMVS, it is

$$W(\omega) = R_d \frac{F(\omega)}{\left(\frac{p}{\omega_d}\right)^{1/2} \sinh\left[\left(\frac{p}{\omega_d}\right)^{1/2}\right]}. \tag{7}$$

The transfer functions of IMPS and IMVS have a common factor $F(\omega)$, and is defined as

$$F(\omega) = \frac{1 - e^{-\alpha d}\left\{e^{(p/\omega_d)^{1/2}} + \left[\left(\frac{p}{\omega_\alpha}\right)^{1/2} - 1\right] \sinh\left[\left(\frac{p}{\omega_d}\right)^{1/2}\right]\right\}}{\left[1 - \frac{p}{\omega_\alpha}\right]}. \tag{8}$$

The absorption coefficient α occurs in Eq. (8) and enables to define the third frequency ω_α,

$$\omega_\alpha = D_n \alpha^2. \tag{9}$$

The extraction of diffusion parameters from the IS is done via the high frequency part of the spectra. There appears a 45° line and a turnover followed by an impedance arc that allows us to extract the diffusion resistance R_d[23] and the diffusion frequency ω_d.[24] This method was widely exploited to obtain the electron diffusion coefficient and electron recombination lifetime in dye-sensitized solar cells.[25–27]

Here, we calculate in Fig. 1 the spectra for the three techniques with the characteristic frequencies obtained from a previous

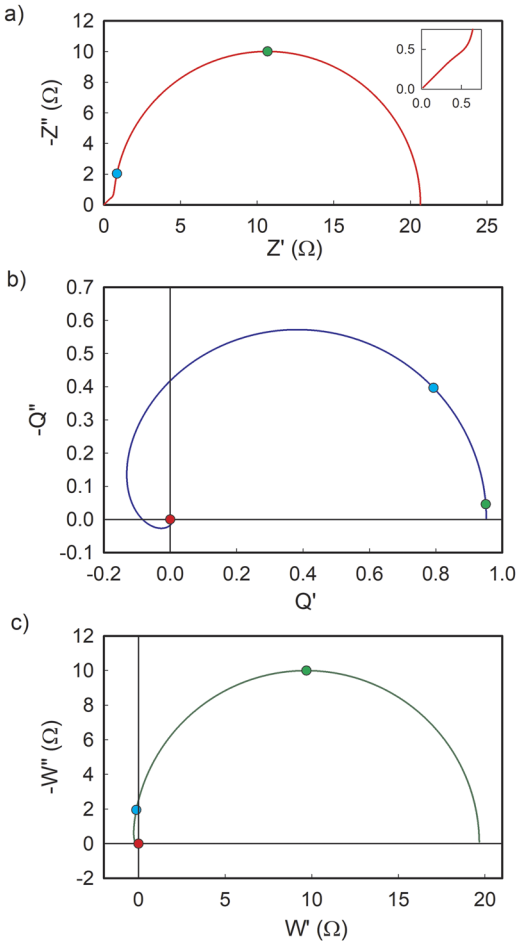

FIG. 1. (a) IS, (b) IMPS, and (c) IMVS spectra for typical values of a carbon-based perovskite solar cell. The values of the parameters are $R_d = 2\Omega$, $\omega_d = 2 \times 10^5 s^{-1}$ (green), $\omega_\alpha = 1 \times 10^8 s^{-1}$ (red), and $\omega_{rec} = 2 \times 10^4 s^{-1}$ (blue). The inset in (a) shows the IS spectrum at high frequency.

study via the data fitting of carbon-based perovskite solar cells.[19] In Fig. 1(a), we see that the 45° line of Eq. (2) indicating the transport resistance appears at a very high frequency but with very small values, due to the high diffusion coefficient of PSC.[28,29] Hence, it has not been possible to distinguish conclusively electron diffusion from other phenomena via the impedance spectra in perovskite solar cells.

However, if we look at the common factor $F(\omega)$ of IMPS and IMVS, the diffusion frequency ω_d appears coupled with ω_α. This opens a door to an alternative pathway to the extraction of diffusion and recombination parameters via light-modulated techniques. In Figs. 1(b) and 1(c), we calculate the IMPS and IMVS spectra for the typical frequency values of carbon-based perovskite solar cells.[19] The coupling of both ω_d and ω_α results in a looping spiral at high frequency crossing the real and/or imaginary axes and going through several quadrants, as shown previously in Refs. 20 and 22. It is important to remark that, as discussed previously in Ref. 20, the IMPS response can be affected by the RC attenuation factor from the series resistance and the geometrical capacitance. However, these RC elements can be extracted from the IS characteristics, and they can be controlled when extracting the diffusion parameters from the IMPS data.

Following these results, we aim to prove these theoretical predictions by the measurement of the three distinct frequency domain small perturbation methods of PSC. However, we note that many different types of spectra are possible. The appearance of the looping spectra in IMPS and IMVS spectra is not a guaranteed result, and neither is the coupling between the frequencies ω_d and ω_α. It has been demonstrated that the loop at high frequency depends on the relationship between these frequencies.[22] This means, experimentally, that the generation inside the perovskite film needs to be non-uniform, i.e., the absorber has to be longer than the absorption length.[20] Therefore, we have chosen carbon-based perovskite solar cells with perovskite film thicknesses above 1 μm and a blue light illumination source that has a short absorption length.[30]

We have measured IS, IMPS, and IMVS at open circuit conditions for a variety of light intensities. The region of interest inside the spectra is in the high frequency domain. Therefore, we have used a Zahner system for the IS that allows up to 10 MHz bias perturbation. However, the results at such high frequencies using standard setups have been proven to be obscured by instrument limitations. Therefore, we have chosen a previously used technique capable of solving these problems and obtaining satisfactory results.[31] To facilitate the correct measurement of current responses at high frequencies, our experimental system uses a current amplifier. This current amplifier introduces an internal series resistance of 50 **Ω** to the extracted current in the IMPS measurements.

We have obtained the expected results for the entirety of the different conditions used, i.e., IS spectra that remain in the positive real part of the complex plane, while the IMPS and IMVS stable

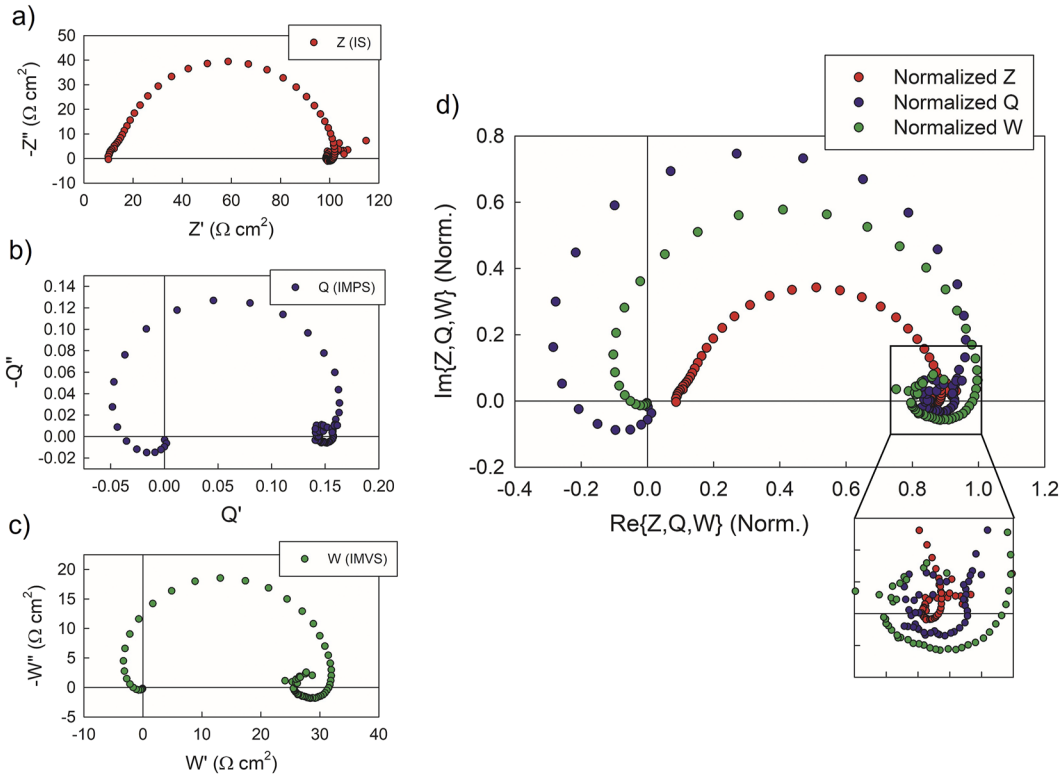

FIG. 2. Experimental complex plane plots of (a) IS, (b) IMPS, and (c) IMVS for a carbon-based perovskite solar cell measured with illumination of 0,11 sun and at open circuit voltage (V = 0.85 V). (d) shows the three normalized spectra together.

responses looped at high frequency crossing the imaginary axis. To illustrate this, we have put together three representative spectra in Fig. 2. The rest of the measured spectra can be found in the supplementary material.

We see in Fig. 2(a) that the IS spectrum draws only a positive real arc where the Warburg element shown in the inset in Fig. 1(a) cannot be distinguished. This can be caused by the interference of other equivalent circuit elements that are orders of magnitude larger than the diffusion resistance.[12,15] Contrarily, both the IMPS and IMVS spectra cross the second quadrant in Figs. 2(b) and 2(c), respectively, clearly showing the effects of diffusion. For the sake of clarity, we show the three spectra in a normalized complex plane plot, in Fig. 2(d), where the shape of the different techniques can be clearly distinguished.

In the combined plot of Fig. 2(d), we see there is a relation in the responses of the three techniques, both in the number of features and in the spectral shape. Previous works have already explained the relationship of the three techniques.[19,32,33] The relationship between IMPS and IMVS transfer functions must give the IS transfer function, as demonstrated in Fig. S1, and following the expression:

$$Z(\omega) = \frac{W(\omega)}{Q(\omega)}. \tag{10}$$

However, none of the previous studies has treated spiral IMPS and IMVS spectra due to ω_d and ω_α coupling. From the expressions of Eqs. (6) and (7), the factor $F(\omega)$, which is the cause of the looping spectra, is canceled by the division, and the IS transfer function is free of this factor. This is a demanding experimental test since the spiraling of the light-modulated spectra of IMPS and IMVS must disappear in the division of Eq. (10). We must show experimentally that the $F(\omega)$ factor is canceled.

As mentioned earlier, the experimental setups for IMPS and IMVS are different from the one we have used for IS. Specifically, a series resistance of 50 **Ω** is introduced by the current amplifier to the extracted current in the IMPS measurements. Therefore, the quotient must be corrected by displacing the points in the complex plane plot 50 **Ω** leftward on the real axis. For further checking that the series resistance only moves the spectra rightward, we have introduced additional series resistances to subsequent IMPS measurements, proving that this is the only effect of the series resistance in the quotient between $W(\omega)$ and $Q(\omega)$. This is clearly seen in Fig. 3(a), where the subsequent addition of a series resistance moves the experimental points of W/Q to the right side of the complex plane. The corrected spectra in Fig. 3(b) show that the experimental quotient (color points) gives a similar response to the experimental IS measured directly (black points). In fact, the looping into the second quadrant gets canceled, therefore, proving that the factor $F(\omega)$ including the ω_α appears neither in the IS response nor in the quotient. We note that the resulting quotient crosses the real axis into the fourth quadrant at high frequency, which is likewise caused by experimental artifacts at the highest frequencies.

Figure 3 confirms that the attainment of diffusion parameters cannot be achieved only by IS, since it is hidden by other phenomena. Therefore, it is convenient to use a combination of techniques, which will allow further extraction of operation

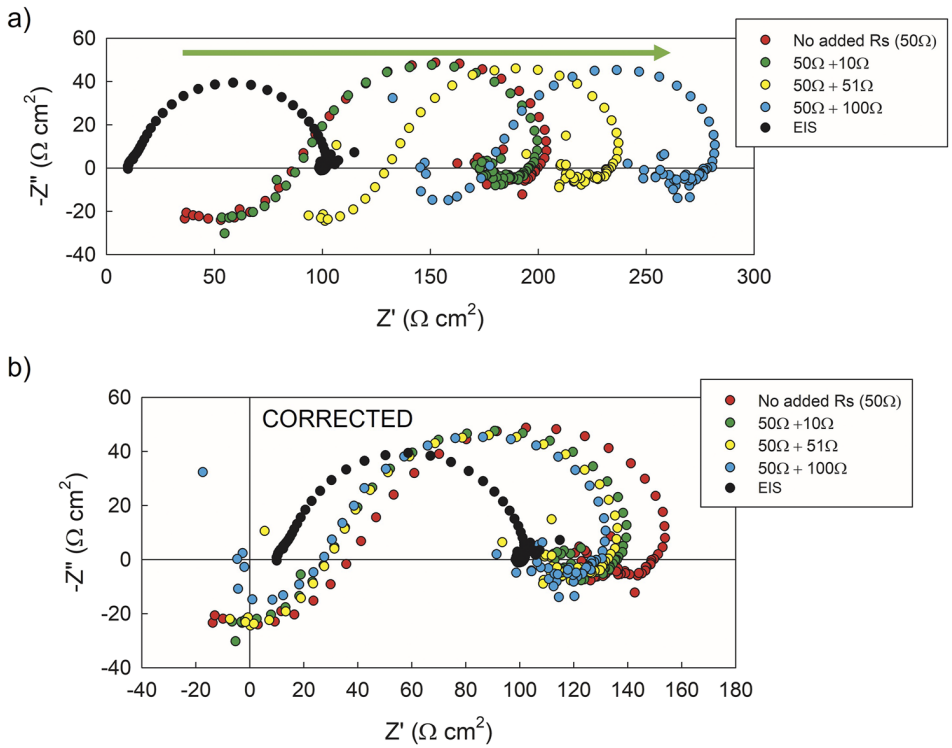

FIG. 3. Experimental complex plane plots of the directly measured IS (black points) and the experimental quotient of IMPS and IMVS given by Eq. (10) (colored points). The IMPS and IMVS measurements include a series resistance of 50 **Ω** from the experimental setup plus added resistances as indicated in the legend. (a) shows the quotients as it is, while (b) shows the corrected spectra by moving leftward the corresponding series resistance value.

parameters. IS is still an important technique, since the series resistance and bulk capacitance obtained at high frequency affect the IMPS response.[20] Hence, a full analysis of perovskite devices requires the utilization of more than one frequency technique with both light and voltage perturbations. In fact, the addition of time-dependent techniques with similar perturbations could bring light on the high frequency response of IMPS and IMVS.[34–36]

In conclusion, although the experimental extraction of diffusion parameters via IS has been achieved in other kind of devices, such as dye-sensitized solar cells, it is not normally possible in perovskite solar cells, due to the infimum feature that it leaves in the IS spectra. However, the obtention of diffusion parameters can be achieved via light-modulated techniques due to the larger spectral trace that is due to the coupling of diffusion and absorption parameters in the high frequency part of the experimental IMPS and IMVS spectra.

The supplementary material includes the experimental details regarding both device fabrication and characterization methods; an extra simulation of both IS and IMVS over IMPS quotient; the current–voltage characteristics of the device; and additional IS, IMPS, and IMVS spectra at different illumination conditions.

We thank Generalitat Valenciana for Project No. PROMETEO /2020/028. A.B. and H.C. acknowledge FPI studentship funding from the Ministerio de Ciencia e Innovación of Spain (Grant Nos. BES-2017-080351 and PRE2020-095374).

AUTHOR DECLARATIONS

Conflict of Interest

The authors have no conflicts to disclose.

DATA AVAILABILITY

The data that support the findings of this study are available within the article and its supplementary material.

REFERENCES

[1] A. Lasia, *Electrochemical Impedance Spectroscopy and Its Applications* (Springer, 2014).
[2] M. E. Orazem and B. Tribollet, *Electrochemical Impedance Spectroscopy*, 2nd ed. (Wiley, 2017).
[3] A. R. C. Bredar, A. L. Chown, A. R. Burton, and B. H. Farnum, "Electrochemical impedance spectroscopy of metal oxide electrodes for energy applications," ACS Appl. Energy Mater. **3**, 66–98 (2020).
[4] Z. Wu, P. Liu, X. Qu, J. Ma, W. Liu, B. Xu, K. Wang, and X. W. Sun, "Identifying the surface charges and their impact on carrier dynamics in quantum-dot light-emitting diodes by impedance spectroscopy," Adv. Opt. Mater. **9**, 2100389 (2021).
[5] S. Taibl, G. Fafilek, and J. Fleig, "Impedance spectra of Fe-doped Srtio3 thin films upon bias voltage: Inductive loops as a trace of ion motion," Nanoscale **8**, 13954–13966 (2016).
[6] F. Fabregat-Santiago, G. Garcia-Belmonte, I. Mora-Seró, and J. Bisquert, "Characterization of nanostructured hybrid and organic solar cells by impedance spectroscopy," Phys. Chem. Chem. Phys. **13**, 9083–9118 (2011).
[7] E. von Hauff, "Impedance spectroscopy for emerging photovoltaics," J. Phys. Chem. C **123**, 11329–11346 (2019).
[8] I. Mora-Seró, G. Garcia-Belmonte, P. P. Boix, M. A. Vázquez, and J. Bisquert, "Impedance spectroscopy characterisation of highly efficient silicon solar cells under different light illumination intensities," Energy Environ. Sci. **2**, 678–686 (2009).
[9] F. Fabregat-Santiago, J. Bisquert, L. Cevey, P. Chen, M. Wang, S. M. Zakeeruddin, and M. Grätzel, "Electron transport and recombination in solid-state dye solar cell with spiro-ometad as hole conductor," J. Am. Chem. Soc. **131**, 558–562 (2009).
[10] Q. Wang, J.-E. Moser, and M. Grätzel, "Electrochemical impedance spectroscopic analysis of dye-sensitized solar cells," J. Phys. Chem. B **109**, 14945–14953 (2005).
[11] B. Arredondo, B. Romero, G. Del Pozo, M. Sessler, C. Veit, and U. Würfel, "Impedance spectroscopy analysis of small molecule solution processed organic solar cell," Sol. Energy Mater. Sol. Cells **128**, 351–356 (2014).
[12] A. Guerrero, G. Garcia-Belmonte, I. Mora-Sero, J. Bisquert, Y. S. Kang, T. J. Jacobsson, J.-P. Correa-Baena, and A. Hagfeldt, "Properties of contact and bulk impedances in hybrid lead halide perovskite solar cells including inductive loop elements," J. Phys. Chem. C **120**, 8023–8032 (2016).
[13] A. Pockett, G. E. Eperon, T. Peltola, H. J. Snaith, A. Walker, L. M. Peter, and P. J. Cameron, "Characterization of planar lead halide perovskite solar cells by impedance spectroscopy, open circuit photovoltage decay and intensity-modulated photovoltage/photocurrent spectroscopy," J. Phys. Chem. C **119**, 3456–3465 (2015).
[14] I. Zarazua, J. Bisquert, and G. Garcia-Belmonte, "Light-induced space-charge accumulation zone as photovoltaic mechanism in perovskite solar cells," J. Phys. Chem. Lett. **7**, 525–528 (2016).
[15] A. Guerrero, J. Bisquert, and G. Garcia-Belmonte, "Impedance spectroscopy of metal halide perovskite solar cells from the perspective of equivalent circuits," Chem. Rev. **121**, 14430–14484 (2021).
[16] S. Ravishankar, O. Almora, C. Echeverría-Arrondo, E. Ghahremanirad, C. Aranda, A. Guerrero, F. Fabregat-Santiago, A. Zaban, G. Garcia-Belmonte, and J. Bisquert, "Surface polarization model for the dynamic hysteresis of perovskite solar cells," J. Phys. Chem. Lett. **8**, 915–921 (2017).
[17] N. Parikh, S. Narayanan, H. Kumari, D. Prochowicz, A. Kalam, S. Satapathi, S. Akin, M. M. Tavakoli, and P. Yadav, "Recent progress of light intensity-modulated small perturbation techniques in perovskite solar cells," Phys. Status Solidi RRL **16**, 2100510 (2021).
[18] S. Ravishankar, C. Aranda, S. Sanchez, J. Bisquert, M. Saliba, and G. Garcia-Belmonte, "Perovskite solar cell modeling using light and voltage modulated techniques," J. Phys. Chem. C **123**, 6444–6449 (2019).
[19] A. Bou, A. Pockett, D. Raptis, T. Watson, M. J. Carnie, and J. Bisquert, "Beyond impedance spectroscopy of perovskite solar cells: Insights from the spectral correlation of the electrooptical frequency techniques," J. Phys. Chem. Lett. **11**, 8654–8659 (2020).
[20] A. Bou, H. Āboliņš, A. Ashoka, H. Cruanyes, A. Guerrero, F. Deschler, and J. Bisquert, "Extracting in situ charge carrier diffusion parameters in perovskite solar cells with light modulated techniques," ACS Energy Lett. **6**, 2248–2255 (2021).
[21] J. Halme, K. Miettunen, and P. Lund, "Effect of nonuniform generation and inefficient collection of electrons on the dynamic photocurrent and photovoltage response of nanostructured photoelectrodes," J. Phys. Chem. C **112**, 20491–20504 (2008).
[22] J. Bisquert and M. Janssen, "From frequency domain to time transient methods for halide perovskite solar cells: The connections of IMPS, IMVS, TPC, and TPV," J. Phys. Chem. Lett. **12**, 7964–7971 (2021).
[23] J. Bisquert, "Theory of the impedance of electron diffusion and recombination in a thin layer," J. Phys. Chem. B **106**, 325–333 (2002).
[24] M. Janssen and J. Bisquert, "Locating the frequency of turnover in thin-film diffusion impedance," J. Phys. Chem. C **125**, 15737–15741 (2021).
[25] Q. Wang, S. Ito, M. Grätzel, F. Fabregat-Santiago, I. Mora-Seró, J. Bisquert, T. Bessho, and H. Imai, "Characteristics of high efficiency dye-sensitized solar cells," J. Phys. Chem. B **110**, 25210–25221 (2006).
[26] J. Bisquert, F. Fabregat-Santiago, I. Mora-Seró, G. Garcia-Belmonte, and S. Giménez, "Electron lifetime in dye-sensitized solar cells: Theory and interpretation of measurements," J. Phys. Chem. C **113**, 17278–17290 (2009).

[27]A. B. F. Martinson, M. S. Goes, F. Fabregat-Santiago, J. Bisquert, M. J. Pellin, and J. T. Hupp, "Electron transport in dye-sensitized solar cells based on zno nanotubes: Evidence for highly efficient charge collection and exceptionally rapid dynamics," J. Phys. Chem. A **113**, 4015 (2009).
[28]S. D. Stranks, G. E. Eperon, G. Grancini, C. Menelaou, M. J. P. Alcocer, T. Leijtens, L. M. Herz, A. Petrozza, and H. J. Snaith, "Electron-hole diffusion lengths exceeding 1 micrometer in an organometal trihalide perovskite absorber," Science **342**, 341–344 (2013).
[29]M. B. Johnston and L. M. Herz, "Hybrid perovskites for photovoltaics: Charge-carrier recombination, diffusion, and radiative efficiencies," Acc. Chem. Res. **49**, 146–154 (2016).
[30]N.-G. Park, "Perovskite solar cells: An emerging photovoltaic technology," Mater. Today **18**, 65–72 (2015).
[31]A. Pockett, M. Spence, S. K. Thomas, D. Raptis, T. Watson, and M. J. Carnie, "Beyond the first quadrant: Origin of the high frequency intensity-modulated photocurrent/photovoltage spectroscopy response of perovskite solar cells," Solar RRL **5**, 2100159 (2021).
[32]L. Bertoluzzi and J. Bisquert, "Investigating the consistency of models for water splitting systems by light and voltage modulated techniques," J. Phys. Chem. Lett. **8**, 172–180 (2017).
[33]A. O. Alvarez, S. Ravishankar, and F. Fabregat-Santiago, "Combining modulated techniques for the analysis of photosensitive devices," Small Methods **5**, 2100661 (2021).
[34]A. Pockett, D. Raptis, S. M. P. Meroni, J. Baker, T. Watson, and M. Carnie, "Origin of exceptionally slow light soaking effect in mesoporous carbon perovskite solar cells with ava additive," J. Phys. Chem. C **123**, 11414–11421 (2019).
[35]L. Krückemeier, B. Krogmeier, Z. Liu, U. Rau, and T. Kirchartz, "Understanding transient photoluminescence in halide perovskite layer stacks and solar cells," Adv. Energy Mater. **11**, 2003489 (2021).
[36]T. Kirchartz, J. A. Márquez, M. Stolterfoht, and T. Unold, "Photoluminescence-based characterization of halide perovskites for photovoltaics," Adv. Energy Mater. **10**, 1904134 (2020).